JOURNAL OF PROPULSION AND POWER
Vol. 23, No. 2, March–April 2007

Magnetohydrodynamic Vortex Containment, Part 3: 1-D Axisymmetric Flow Model

Raymond J. Sedwick* and Daniel A. Zayas†
Massachusetts Institute of Technology, Cambridge, Massachusetts 02139

DOI: 10.2514/1.19726

This is the third in a series of papers on research conducted on magnetohydrodynamically driven vortex containment for gas core nuclear propulsion. This paper takes the chemical, electrical, and optical properties of the propellant/fuel mixture derived in the previous work and uses them in a 1-D axisymmetric flow model to assess the effectiveness of using MHD to improve fuel confinement in the vortex. Governing equations for mass, momentum, and energy transport are derived, and reduced to dimensionless forms. Some of the free parameters in the system design are constrained based on physical considerations, whereas others are constrained through optimization. The opacity of the fuel/propellant mixture permits the use of a diffusive equation for radiative heat transfer, and the results show that this transfer to the outer walls of the vortex is not the limiting factor in performance as is often assumed. However, requirements on limiting the uranium loading at the outer walls are found to fundamentally limit the allowable heating rate within the vortex. As a consequence, the core temperature is shown to be limited to around 5000 K, and the specific impulse to around 1200–1500 s.

Nomenclature

$\boldsymbol{B}$	=	magnetic field vector
c_p	=	specific heat capacity
D_{12}	=	H–U diffusion coefficient
E	=	total energy
$\boldsymbol{E}$	=	electric field vector
g	=	gravitational acceleration
g'	=	volumetric heating term
H	=	total enthalpy
h	=	enthalpy
h	=	Planck constant
I_{sp}	=	specific impulse
$\boldsymbol{J}$	=	electric current vector
K_M	=	concentration coefficient
k	=	Boltzmann constant
$\mathcal{M}$	=	total mass flow rate per length
M_{tm}	=	tangential Mach number
$\mathcal{M}_1$	=	hydrogen mass flow rate per length
$\mathcal{M}_2$	=	uranium mass flow rate per length
m	=	molecular weight
N_A	=	Avogadro's number
n	=	number density
$\mathcal{P}$	=	power per unit vortex length
p	=	pressure
Q	=	energy per fission
$\dot{q}$	=	heat flux
$\boldsymbol{q}$	=	heat flux vector
R	=	specific ideal gas constant
$\mathcal{R}$	=	universal ideal gas constant
r	=	radius
T	=	temperature
u	=	radial velocity
v	=	tangential velocity
w	=	uranium loading
w_c	=	vortex core uranium loading
y	=	mass fraction
θ_v	=	characteristic vibrational temperature
κ_r	=	Rosseland mean opacity
λ_c	=	conduction coefficient
λ_r	=	radiative conduction coefficient
ρ	=	density
σ	=	conductivity
σ_f	=	fission cross section
ϕ	=	neutron flux

Received 28 August 2005; revision received 18 May 2006; accepted for publication 31 May 2006.

*Principal Research Scientist, Department of Aeronautics and Astronautics, Space Systems Laboratory; sedwick@mit.edu. Senior Member AIAA.

†Graduate Research Fellow, Department of Aeronautics and Astronautics, Space Systems Laboratory. Member AIAA.

Introduction

IT was first conceived in 1957 that the pressure gradients present in a hydrodynamic vortex could provide a mechanism to contain a hot reacting fuel within a flowing propellant [1]. Studies showed that this approach was initially quite attractive. A distribution of uranium that had low density at the outer wall and inner core, and peaked at some radius in between would in theory limit uranium loss and wall heating, while still providing ample heat transfer to the propellant. However, fairly extensive experimental and theoretical studies revealed problems with turbulent shear and subsequent mixing at the high Reynolds numbers required for containment, leading to vortex strengths that could never meet the requirements. To alleviate the problem, it was theorized that electromagnetic forces could be employed to strengthen the vortex, independent of the mass flow rate. An electrical circuit would be created between the outer circumferential wall of the vortex tube and the center of the forward wall (opposite the nozzle; see Fig. 1). The high temperature of the fuel would provide sufficient ionization (conductivity) along the axis that the primary component of the electric field would be radial. In addition, an axial magnetic field would be established by wrapping a coil around the outer perimeter of the tube. The $\boldsymbol{E} \times \boldsymbol{B}$ drift of the current would then be azimuthal, and the high collisionality within the vortex would mean that this force was transferred to the propellant, strengthening the vortex.

Whether gas phase fuel containment is possible can be determined in first approximation by an analysis of the radial flow field of the vortex tube. The two key issues that must be addressed are 1) keeping the fuel away from the core of the vortex where high axial velocities will carry it out of the nozzle, and 2) isolating the outer wall from the large internal heat flux. Because of the axisymmetric nature of the flow field, variations in the azimuthal direction are assumed to be zero, however, the azimuthal momentum equation is still maintained.

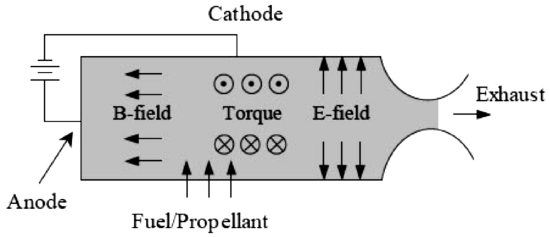

Fig. 1 Schematic of MHD-driven vortex.

It is for this reason that the model is referred to as "quasi 2-D." It is also assumed that the only species present are U, U^+, H_2, H, H^+, and e^-, because it has been determined that the fluorine levels in the system will be low, if not zero [2,3]. Finally, for the analysis performed, the flow is assumed inviscid, because earlier analysis [1] demonstrated that the uranium concentration will drop to low levels well outside of the central viscous layer of the vortex.

Governing Equations

Mass Conservation Equations

The mass conservation analysis starts with the axisymmetric equations of continuity. Each of the species must satisfy its own continuity equation, and together they must satisfy a global equation. The total mass flow rate of hydrogen (including H_2, H, and H^+) per unit vortex length is given by $\mathcal{M}_1$, and the analogous quantity for the uranium (both U and U^+) is given by $\mathcal{M}_2$. The general form of the mass conservation equation is

$$\frac{\partial}{\partial t}(\rho) + \nabla \cdot (\rho \boldsymbol{u}) = 0 \tag{1}$$

and under the assumption of steady state, 1-D axisymmetric flow simplifies to

$$\frac{1}{r}\frac{\mathrm{d}}{\mathrm{d}r}(\rho u r) = 0 \tag{2}$$

Integrating this equation shows that $\rho u r$ is a constant that depends on the species under consideration. In this form, the three equations of continuity become

$$\mathcal{M}_1 = 2\pi\rho_1(u + u_1)r \qquad \mathcal{M}_2 = 2\pi\rho_2(u + u_2)r$$
$$\mathcal{M} = 2\pi\rho u r \tag{3}$$

where u_1 and u_2 are the radial diffusion velocities of the hydrogen and the uranium, respectively.

For the flow of a mixture, the diffusion velocity of each species is a result of the differential push of the global pressure gradient, the redistribution due to each species partial pressure gradient and the difference in thermal velocity resulting from the temperature gradient. Regarding the thermal diffusion as small compared with the other effects [1], the radial diffusion velocity of species 2 in a two species flow is given in one form by [4]

$$u_2 = -D_{12}\frac{\rho_1}{\rho}\left[\frac{n}{n_1}\frac{\mathrm{d}\log(n_2/n)}{\mathrm{d}r} + \frac{n(m_1 - m_2)}{\rho}\frac{\mathrm{d}\log p}{\mathrm{d}r}\right] \tag{4}$$

with D_{12} as the binary diffusion coefficient, n the number density, and m the molecular mass of the species. Because of the large number of hydrogen atoms as compared with the uranium and fluorine, it can be assumed that the diffusion of each of the lower concentration species is affected only by the hydrogen, and not by the other species. In this way, all diffusion processes can be treated as binary, and the above relationship can be used. The diffusion velocity u_1 can be found by eliminating u from Eq. (3) resulting in $\rho_1 u_1 + \rho_2 u_2 = 0$.

Momentum Conservation Equations

Beginning once again with the vector representation, the momentum conservation equation is given as

$$\frac{\partial}{\partial t}(\rho \boldsymbol{u}) + \nabla \cdot (\rho \boldsymbol{u}\boldsymbol{u}) + \nabla p = \boldsymbol{J} \times \boldsymbol{B} \tag{5}$$

where the electromagnetic body force per unit volume on the fluid appears on the right side of the equation. Again, under the assumption of steady, inviscid, 1-D axisymmetric flow, the radial and azimuthal momentum equations are

$$\frac{1}{r}\frac{\mathrm{d}}{\mathrm{d}r}(\rho u^2 r) + \frac{\mathrm{d}p}{\mathrm{d}r} - \frac{\rho v^2}{r} = 0 \qquad \frac{1}{r}\frac{\mathrm{d}}{\mathrm{d}r}(\rho u v r) + \frac{\rho u v}{r} = J_r B_z \tag{6}$$

where a radial current and an axial B field are applied to generate only an azimuthal body force, and v is introduced as the azimuthal velocity component. To maintain the distribution of uranium within the vortex, the radial flow velocity must be on the order of the diffusion velocity, and, consequently, u is much lower than v for effective containment. The only point at which this assumption would not necessarily hold would be at the outer boundary, where turbulent mixing and wall shear require that the azimuthal velocity be at a low value compared with the injection velocity. The effect would be a small error in the pressure gradient very close to the outer wall, and will be ignored. From this, terms of u can be neglected relative to terms of v in the radial momentum equation, and applying total mass conservation to the azimuthal momentum equation yields

$$\frac{\mathrm{d}p}{\mathrm{d}r} - \frac{\rho v^2}{r} = 0 \qquad \frac{\rho u}{r}\frac{\mathrm{d}}{\mathrm{d}r}(v r) = J_r B_z \tag{7}$$

Defining w to be the mass density ratio of uranium to hydrogen, it is assumed as before that the number density of uranium will always be much less than that of hydrogen, and the ideal gas law can then be used to eliminate the density from the above equation. This yields

$$\frac{\mathrm{d}\,\ell_n\, p}{\mathrm{d}\,\ell_n\, r} = \frac{(1 + w)v^2}{RT} \tag{8}$$

This expression can then be substituted into Eq. (3) along with the continuity equations to eliminate the densities. The result is a first order differential equation for the variation of w across the vortex

$$1 - \left(\frac{1 + w}{w}\right)\left(\frac{\mathcal{M}_2}{\mathcal{M}}\right) = \frac{2\pi\rho_1 D_{12}}{\mathcal{M}}\left[\frac{\mathrm{d}\,\ell_n\, w}{\mathrm{d}\,\ell_n\, r} - \left(\frac{m_2}{2 - y} - 1\right)\frac{v^2}{RT}\right] \tag{9}$$

Returning to the azimuthal momentum equation, the electromagnetic force term $J_r B_z$ is replaced by $-JB$, where the current and magnetic field directions have been chosen to increase the angular momentum as the radius decreases. From Maxwell's equations, $\nabla \cdot \boldsymbol{J} = 0$ in the absence of a time varying charge density (steady state), which in the case of axisymmetry indicates that $Jr =$ constant. This constant can be specified using $\mathcal{I} = 2\pi r J$ for the current per unit vortex length. The azimuthal momentum equation then becomes

$$\frac{\mathrm{d}}{\mathrm{d}r}(v r) = -\left(\frac{\mathcal{I}B}{\mathcal{M}}\right)r \tag{10}$$

where the continuity equation has been used to eliminate ρu. This equation directly demonstrates the utility of adding the electromagnetic fields to the flow. Whereas before the product (vr) would have remained constant (conservation of angular momentum), it now increases with decreasing radius as a result of the electromagnetic force that pushes each unit volume in the $\boldsymbol{J} \times \boldsymbol{B}$ direction as it flows inward. This equation can now be integrated to yield

$$(vr)_2 - (vr)_1 = \frac{IB}{2\dot{m}}(r_1^2 - r_2^2) \tag{11}$$

where 1 and 2 refer to positions in the flow, and the ratio $\mathcal{I}/\mathcal{M}$ has been replaced by $I/\dot{m}$ (the ratio of total current to mass flow rate) under the assumption of uniform mass flow along the vortex length. This gives an expression for the azimuthal velocity that depends only on constants of the vortex and the radius. Now all that is necessary is a relationship that will yield the temperature across the vortex.

Energy Conservation Equation

Starting once again with the vector representation, the expression for energy conservation in the presence of general volumetric heat addition is given as

$$\frac{\partial}{\partial t}(\rho E) + \nabla \cdot [\rho H \boldsymbol{u}] + \nabla \cdot \boldsymbol{q} = g' + \boldsymbol{J} \cdot \boldsymbol{E} \tag{12}$$

where $\boldsymbol{J} \cdot \boldsymbol{E}$ is the contribution from Ohmic heating, and (g') contains the rest. Under the current set of assumptions this then becomes

$$\frac{1}{r}\frac{\mathrm{d}}{\mathrm{d}r}[\rho u r h] + \rho u \frac{\mathrm{d}}{\mathrm{d}r}\left(\frac{u^2+v^2}{2}\right) + \frac{1}{r}\frac{\mathrm{d}}{\mathrm{d}r}(qr) = g' + JBv + \frac{J^2}{\sigma} \tag{13}$$

by separating the kinetic energy from the total enthalpy and using a simplified form of the generalized Ohm's Law, $J = \sigma(\boldsymbol{E} + \boldsymbol{v} \times \boldsymbol{B})$, to express E in terms of J and the back emf $\boldsymbol{v} \times \boldsymbol{B}$. Returning now to the original form of the momentum equations [Eq. (6)], the continuity equation may be used to pull the constant product $\rho u r$ from the derivatives. Multiplying the radial momentum equation by u and the azimuthal momentum equation by v, they may be added and rearranged to give

$$\rho u^2 \frac{\mathrm{d}u}{\mathrm{d}r} + \rho u v \frac{\mathrm{d}v}{\mathrm{d}r} = JBv - u\frac{\mathrm{d}p}{\mathrm{d}r} \tag{14}$$

the LHS of which is identical to what is obtained by differentiating the kinetic energy term in the energy equation [Eq. (13)]. Making this substitution yields the internal energy equation

$$\frac{1}{r}\frac{\mathrm{d}}{\mathrm{d}r}[\rho u r h] = u\frac{\mathrm{d}p}{\mathrm{d}r} - \frac{1}{r}\frac{\mathrm{d}}{\mathrm{d}r}(rq) + g \tag{15}$$

where $q = \lambda(\mathrm{d}T/\mathrm{d}r) + h_2 u_2 - h_1 u_1$ contains the diffusive heat transfer mechanisms, with λ as the heat conductivity. The last term (g) is the modified volumetric rate of heat addition, which now includes the Ohmic heating term, J^2/σ. The back emf term has been canceled by the substitution of the momentum equations. In the previous work by Kerrebrock and Meghreblian, the collisional heat conduction was shown to be negligible over a large portion of the flow and was therefore dropped. This approximation was most convenient in that it reduced the energy equation to first order, and is therefore maintained for this analysis. The validity of this will be demonstrated in the numerical results to be presented later. The convective terms of the separate species on the right can be combined with the LHS to give

$$\frac{1}{r}\frac{\mathrm{d}}{\mathrm{d}r}[\rho_1(u+u_1)h_1 r + \rho_2(u+u_2)h_2 r] = u\frac{\mathrm{d}p}{\mathrm{d}r} + g \tag{16}$$

Substituting the equations of continuity [Eq. (3)] and the pressure gradient [Eq. (7)] and performing the differentiation, the energy equation may be cast in the following form:

$$\frac{\mathcal{M}_1}{\mathcal{M}}\frac{\mathrm{d}h_1}{\mathrm{d}r} + \frac{\mathcal{M}_2}{\mathcal{M}}\frac{\mathrm{d}h_2}{\mathrm{d}r} = \frac{v^2}{r} + \frac{2\pi r}{\mathcal{M}}g \tag{17}$$

From this it is seen that the total change of the enthalpies per unit mass of the two gases across the vortex is equal to the sum of the work done by the spatially varying pressure field and the energy per unit mass added to the flow at each point. Realizing $\mathcal{M}$ is negative (directed radially inward) it is also seen that the heat added increases the enthalpy as r decreases, or equivalently, the slope $\mathrm{d}T/\mathrm{d}r$ is less than zero for heat addition. Without the volumetric heat addition, the static enthalpy (or the temperature) would decrease toward the center as energy is converted from thermal to kinetic.

Following an argument by Kerrebrock and Meghreblian regarding the exit boundary condition it was concluded that the ratio of uranium mass flow to hydrogen mass flow is upper bounded by the relative concentrations of the two at the outflow boundary, as if a porous cylinder were located there. Because of the positive pressure gradient that still exists at the "core" boundary of the vortex, the uranium will have an outward diffusion velocity relative to the mean mass flow. In the limit of zero relative velocity, the mass flow ratio would exactly equal the concentration ratio, which is why this condition represents an upper bound. The situation is not the same at the inflow boundary because mixing occurs. Consequently, if the density of uranium to hydrogen at the inner boundary (the core) is designated w_c, the upper-bound ratio of uranium to hydrogen mass flow can be expressed as

$$\frac{\mathcal{M}_2}{\mathcal{M}} = \frac{w_c}{1+w_c} \tag{18}$$

Because the relative concentration of the uranium is set to an arbitrarily small value (10^{-4}) at this point, terms involving $\mathcal{M}_2$ may be eliminated (as compared with $\mathcal{M}_1$) provided all other factors are of the same order, and the approximation made that $\mathcal{M} \approx \mathcal{M}_1$. Also, because the specific heat per unit mass of uranium is even less than that of hydrogen (due to their relative masses), the second term is justifiably discarded from the LHS of Eq. (17) leaving only the enthalpy flux of the hydrogen. The resulting form of the energy equation is then

$$\frac{\mathrm{d}h_1}{\mathrm{d}r} = \frac{v^2}{r} + \frac{2\pi r}{\mathcal{M}}g \tag{19}$$

neglecting the contribution of electrons to convection.

Convection

Convection is examined by first rewriting the spatial derivative of the enthalpy using the chain rule as

$$\frac{\mathrm{d}h}{\mathrm{d}r} = \frac{\mathrm{d}h}{\mathrm{d}T}\frac{\mathrm{d}T}{\mathrm{d}r} \tag{20}$$

and using predeveloped expressions for the specific heats of the electrons and hydrogen species. The left side of Eq. (19) can then be written as [3]

$$\left[\frac{5}{2}y + \left\{\frac{7}{2} + \left(\frac{\theta_v/2T}{\sinh(\theta_v/2T)}\right)^2\right\}\frac{1-y}{2}\right]\mathcal{R}\frac{\mathrm{d}T}{\mathrm{d}r} \tag{21}$$

By the same argument, one may ask if the electrons, having such a high mass specific heat, may contribute significantly to the convection of heat across the vortex. The electric current level necessary to have a substantial contribution can be easily determined by imposing that the convective heat flux from the electrons be of the same order of magnitude as that of the hydrogen. This implies

$$\frac{\rho_e h_e u_e}{\rho_H h_H u_H} = \frac{\rho_e c_{pe} u_e}{\rho_H c_{pH} u_H} \sim 1 \tag{22}$$

and putting the mass flow of the electrons in terms of the electric current, $J = e n_e u_e$, the required current level can be expressed in terms of the propellant flow rate as

$$J \sim \frac{e N_A \mathcal{M}}{2\pi r m_H} \tag{23}$$

It will be seen later that the current levels present in the system will not in fact be high enough for the electron motion to contribute to convective heat transfer. The remaining mechanisms of heat transfer are contained within the volumetric heat addition term (g), and are 1) Ohmic heating, 2) electromagnetic radiation, and 3) nuclear fission.

Ohmic Heating

It was seen in the development of Eq. (15) that there is no contribution to the volumetric heating from the back emf, leaving only the term J^2/σ. Using the current continuity equation gives a constant value of the product Jr, and thus the evaluation of the Ohmic heating becomes straightforward. The conductivity depends on both electron number density and collision frequency. Although

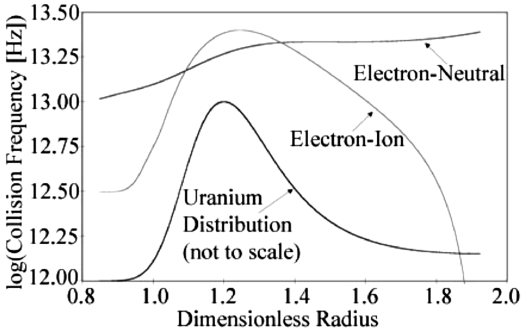

Fig. 2 Electron collision frequency with ions and neutrals.

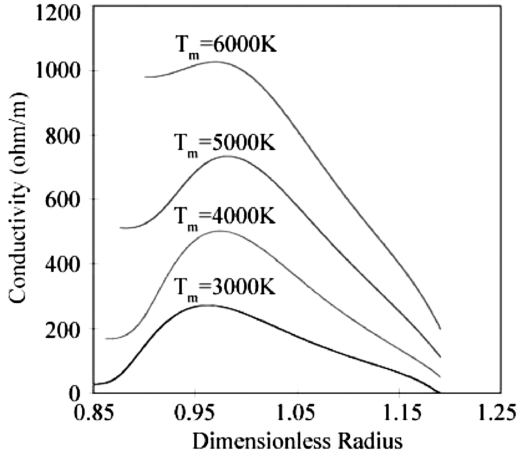

Fig. 3 Conductivity versus radius.

the cross section of electron-ion collisions is 1–2 orders of magnitude larger than electron-neutral, most of the ions and electrons are the result of uranium ionization, which is present in molar concentrations that are much lower than the propellant. Figure 2 shows that the electron-neutral collision frequency is actually dominant over much of the vortex, except when both the concentration of uranium and the temperature are relatively high. Because the electron-neutral cross-section is nearly constant across the vortex, the conductivity very closely follows the uranium distribution. This can be seen in Fig. 3.

Radiation

In determining the rate at which energy is transferred radiatively at various points in the system, several factors come into play. The opacity increases with temperature (toward the core), the overall density increases with radius, and the uranium density ratio peaks somewhere in between. The optical depth per unit length depends on the product

$$\kappa\rho_u = \frac{\kappa p w}{\mathcal{R}T}\left[\frac{1}{2-y}+\frac{w}{m_U}\right]^{-1} \tag{24}$$

and is plotted in Fig. 4 along with the temperature and uranium concentration for a 5,000 K peak temperature. The maximum optical depth per unit length is shown to be 160 cm^{-1}, and drops to roughly 110 cm^{-1} at the peak uranium distribution. The only point in the vortex where the optical depth per unit length drops to a level where radiation may travel significant distances is in the core. Because only radiation emitted close to the wall will arrive there, the wall will "see" a gas that is only slightly elevated in temperature, and be shielded from the high temperature core. The radiation in the core will effectively be trapped radially by the uranium distribution as is desired.

As a result of the optically thick nature of the gas a diffusive approximation to radiative heat transfer is justified. Drawing an analogy to the treatment of heat conduction, one starts with an

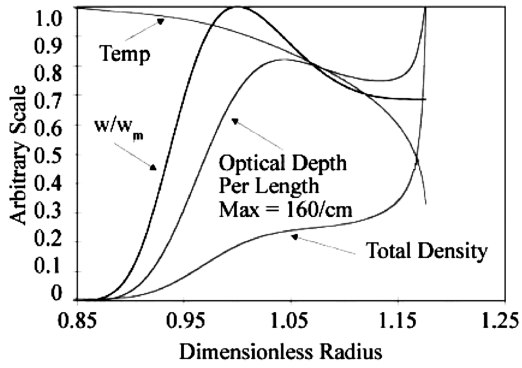

Fig. 4 Optical depth per length vs radius.

expression for the power transferred across a unit area. For conduction this is the Fourier Law, which depends on the gradient of the temperature, $\dot{q}_c = -\lambda_c \nabla T$. The divergence of this quantity gives the net amount of heat leaving an element of volume per unit time due to the flux of power through its walls. The analogous expression for radiation has a λ_r that is strongly dependent on T, and hence the volumetric heat addition by radiation in 1-D axisymmetric coordinates is then

$$g_{\text{rad}} = \left(\frac{\mathrm{d}\lambda_r}{\mathrm{d}r}+\frac{\lambda_r}{r}\right)\frac{\mathrm{d}T}{\mathrm{d}r}+\lambda_r\frac{\mathrm{d}^2T}{\mathrm{d}r^2} \tag{25}$$

It is seen that three terms appear, where two have been grouped together for the purpose of illustration. These two terms are proportional to the slope of the temperature and hence act in the same way as the mass convection terms. The third term is proportional to the second derivative of the temperature, and appears in the same form as the usual heat conduction, acting as a volumetric heat source. These terms will be addressed when the full energy equation is made dimensionless.

Fission

The final component of the volumetric heating term accounts for heat generated from the fission of the uranium fuel. Although it is the primary source of heating in the system, it is considered at the end due to the special way it is to be treated. The analysis begins by finding the functional dependence of the system on the physical parameters. The power produced per unit volume is given by $g_{\text{fiss}} = Q\sigma_f\phi n_2$, which is the product of the energy per fission, fission cross section, neutron flux and uranium particle density, respectively. This can be written in terms of the local pressure, temperature, and uranium concentration, and provided that w_m is at maximum of order 10 (which is the case), can be approximated by

$$g_f \approx \left(\frac{Q\sigma_f\phi}{k}\frac{(2-y)}{m_2}\right)\frac{pw}{T} \tag{26}$$

A maximum heating value exists [1,2], above which no maximum fuel concentration is generated away from the outer boundary. A similar value exists in the presence of Ohmic heating and radiation, and will be found after the equations are nondimensionalized. The heat addition from fission will then be considered parametrically by varying the fraction of the maximum heating value that is used, rather than specifying the neutron flux. For a given fraction of the maximum, the necessary neutron flux can be easily calculated. After some algebraic manipulation, the full energy equation can now be written as

$$\left[yc_{p_H}+(1-y)c_{p_{H_2}}-\frac{2\pi r}{\mathcal{M}}\left(\frac{\mathrm{d}\lambda_r}{\mathrm{d}r}+\frac{\lambda_r}{r}\right)\right]\frac{\mathrm{d}T}{\mathrm{d}r} = \frac{v^2}{r}+\frac{2\pi r}{\mathcal{M}}\left(g_f+g_o+\lambda_r\frac{\mathrm{d}^2T}{\mathrm{d}r^2}\right) \tag{27}$$

and the system of governing equations may now be nondimensionalized.

Nondimensionalized Equations

The governing equations take on a more illustrative and general form if they are functions of dimensionless parameters and boundary conditions. As in the previous work [1], equations of the following form are sought

$$\frac{\mathrm{d}T^*}{\mathrm{d}r^*} = f_1(T^*, w, p^*, r^*, M_{\mathrm{tm}}, w_m, \boldsymbol{g}_m)$$
$$\frac{\mathrm{d}w}{\mathrm{d}r^*} = f_2(T^*, w, r^*, w_m, M_{\mathrm{tm}}) \qquad \frac{\mathrm{d}p^*}{\mathrm{d}r^*} = f_3(T^*, w, r^*, M_{\mathrm{tm}}) \tag{28}$$

where the variables T, p, and r are nondimensionalized with respect to their values at the maximum of w (w_m), and M_{tm} and $\boldsymbol{g}_m$ are the tangential Mach number and volumetric heat addition values at this same point. The boundary conditions (applied to this same point) take the simple form

$$T^*(1) = 1, \qquad p^*(1) = 1, \qquad w(1) = w_m \tag{29}$$

The nondimensionalization begins with Eq. (11) for azimuthal velocity, which is first written in terms of Mach number using the local speed of sound. The ratio of sound speeds is then reduced to temperature and molecular weight ratios related to the maximum uranium concentration point as follows:

$$M_t = \frac{M_{\mathrm{tm}}}{r^* T^{*1/2}} \left(\frac{2-y}{2-y_m}\right)^{1/2} [1 + \mathrm{MHD}(1 - r^{*2})] \tag{30}$$

where the first dimensionless parameter MHD is given by

$$\mathrm{MHD} = \frac{IBr_m}{2\dot{m}v_m} \tag{31}$$

and can be interpreted as the ratio of applied torque to angular momentum flux at the peak fuel concentration radius. The equation for the pressure variation will be the same as in the original work, because writing it in terms of the Mach number has already removed the dimension of all right hand terms, and the molecular weight is contained within its definition. From Eq. (8) is then obtained

$$\frac{\mathrm{d}\,\ell n\, p^*}{\mathrm{d}\,\ell n\, r^*} = \gamma M_t^2 (1 + w) \tag{32}$$

where M_t is given previously. Similarly for the uranium concentration, given by Eq. (9), the dependence of the binary diffusion coefficient on the flow properties is determined. From the simple result based on hard sphere collisions, the expression is given by [4]

$$D_{12} = \frac{3}{8nd_{12}^2} \left[\frac{(m_1 + m_2)kT}{2\pi m_1 m_2}\right]^{1/2} \tag{33}$$

The product $\rho_1 D_{12}$ in Eq. (9) can be nondimensionalized using this equation, resulting in the relationship

$$(\rho_1 D_{12}) = (\rho_1 D_{12})_m T^{*-1/2} \tag{34}$$

and an expression for $(\rho_1 D_{12})_m$ is found by evaluating Eq. (9) at the peak concentration radius. Because at this point $(1 + w_m)/w_m$ is of order unity, $\mathcal{M}_2/\mathcal{M} \ll 1$, and the slope of $\mathrm{d}w/\mathrm{d}r = 0$ by definition, this expression becomes

$$(\rho_1 D_{12})_m = -\frac{\mathcal{M}}{2\pi} \left[\left(\frac{m_2}{2-y} - 1\right) \frac{v^2}{RT}\right]^{-1} \tag{35}$$

Equations (34) and (35) may then be substituted into Eq. (9) to yield

$$\frac{\mathrm{d}\,\ell n\, w}{\mathrm{d}\,\ell n\, r} = \left(\frac{m_2}{2-y} - 1\right) \frac{v^2}{RT} \left\{1 - \frac{1}{T^{*1/2}} \frac{(\frac{m_2}{2-y_m} - 1)}{(\frac{m_2}{2-y} - 1)} \frac{v_m^2}{R_m T_m} \frac{RT}{v^2} \times \left[1 - \left(\frac{1+w}{w}\right)\left(\frac{w_c}{1+w_c}\right)\right]\right\} \tag{36}$$

Expressing the velocities in terms of Mach numbers, and using the fact that $m_2/(2 - y_m) \gg 1$ for all y, this result can be written as

$$\frac{\mathrm{d}\,\ell n\, w}{\mathrm{d}\,\ell n\, r^*} = \frac{\gamma_m M_{\mathrm{tm}}^2 m_2}{2 - y_m} \left\{\frac{\gamma M_t^2}{\gamma_m M_{\mathrm{tm}}} \left(\frac{2-y_m}{2-y}\right) - \frac{1}{T^{*1/2}} \left[1 - \left(\frac{1+w}{w}\right)\left(\frac{w_c}{1+w_c}\right)\right]\right\} \tag{37}$$

and Eq. (30) can be used to express M_{tm}^2/M_t^2 in terms of other quantities.

Finally, making the energy equation dimensionless yields

$$\left[\frac{c_{p_H}}{\mathcal{R}} y + \frac{c_{p_{H_2}}}{\mathcal{R}} (1 - y) + g_{\mathrm{rad}_m} \left(r^* \frac{\mathrm{d}\lambda_r^*}{\mathrm{d}r^*} + 1\right)\right] \frac{\mathrm{d}T^*}{\mathrm{d}r^*} = \frac{T^*(2 - y_m)}{r^*(2 - y)} \gamma M_t^2 - g_{\mathrm{rad}_m} r^* \lambda_r^* \frac{\mathrm{d}^2 T^*}{\mathrm{d}r^{*2}} - g_{\mathrm{fiss}_m} \frac{(2-y)}{(2-y_m)} \frac{p^* r^* w}{T^* w_m} - g_{\mathrm{Ohm}_m} \frac{1}{\sigma^* r^*} \tag{38}$$

where the dimensionless volumetric heating parameters have been defined as follows:

$$g_{\mathrm{fiss}_m} = \left(\frac{2\pi r_m^2 Q \sigma_f \phi}{k|\mathcal{M}|\mathcal{R}T_m} \frac{(2-y_m)}{m_2} \frac{p_m w_m}{T_m}\right) \tag{39}$$

$$g_{\mathrm{rad}_m} = \left(\frac{2\pi \lambda_{r_m}}{|\mathcal{M}|\mathcal{R}}\right) \tag{40}$$

$$g_{\mathrm{ohm}_m} = \left(\frac{2\pi (r_m J_m)^2}{T_m \sigma_m |\mathcal{M}|\mathcal{R}}\right) \tag{41}$$

It should be noted that the absolute value of the mass flow per unit vortex length appears within the volumetric heating parameters, and the corresponding signs in the energy equation have been changed to reflect this.

Radiation Dilemma

As mentioned earlier, there is a maximum heating rate that can be supplied by nuclear fission if an extremum (maximum) is to occur in the uranium mass fraction distribution. The condition on this particular heating rate was that the dimensionless slope of the temperature ($\mathrm{d}T^*/\mathrm{d}r^*$) has a value of -4 at the extremum point [1,2]. For heating rates below the maximum, the dimensionless slope will have a larger value (more positive). Equation (38) can be written at r_m as

$$g_{\mathrm{fiss}_m} = -g_{\mathrm{rad}_m} \left(\frac{\mathrm{d}^2 T^*}{\mathrm{d}r^{*2}}\right)_m - \left\{\frac{c_{p_m}}{\mathcal{R}} + g_{\mathrm{rad}_m} \left[\left(\frac{\mathrm{d}\lambda_r^*}{\mathrm{d}r^*}\right)_m + 1\right]\right\} \left(\frac{\mathrm{d}T^*}{\mathrm{d}r^*}\right)_m \tag{42}$$

where the cooling due to expansion and Ohmic heating have been removed because they are small relative to other terms at this point in the flow. This equation states that there is one dominant source of heat generation, and two mechanisms of heat transfer. Heat is of course generated by fission, which is represented by the term on the LHS of the energy equation. Heat transfer is performed by both the convection of energy by mass transfer, and radiation of energy by electromagnetic waves. In the opaque gas regime, the radiative transfer has characteristics of both conduction and convection. The conduction term is proportional to the second derivative of the temperature, and the convective term is proportional to the first.

Recalling that λ_R is defined as [2]

$$\lambda_R = \frac{16\sigma T^3}{3\rho_u \kappa_r} \tag{43}$$

taking the natural log of this expression and differentiating with respect to radius results in

$$\frac{1}{\lambda_r}\frac{\mathrm{d}\lambda_r}{\mathrm{d}r} = \frac{3}{T}\frac{\mathrm{d}T}{\mathrm{d}r} - \frac{1}{\rho_u}\frac{\mathrm{d}\rho_u}{\mathrm{d}r} - \frac{1}{\kappa_r}\frac{\mathrm{d}\kappa_r}{\mathrm{d}r} \tag{44}$$

which can then be nondimensionalized and evaluated at r_m to obtain

$$\left(\frac{\mathrm{d}\lambda_r^*}{\mathrm{d}r^*}\right)_m = 3\left(\frac{\mathrm{d}T^*}{\mathrm{d}r^*}\right)_m - \left(\frac{\mathrm{d}\rho_u^*}{\mathrm{d}r^*}\right)_m - \left(\frac{\mathrm{d}\kappa_r^*}{\mathrm{d}r^*}\right)_m \tag{45}$$

The uranium density can be written in terms of the overall density as

$$\rho_u = \frac{w}{1+w}\rho \tag{46}$$

and using the ideal gas law to express the overall density in terms of the pressure and temperature yields

$$\rho_u = \left[\frac{w m_u m_H}{m_u + w m_H}\right]\frac{p}{\mathcal{R}T} \tag{47}$$

Again, taking the log of this expression, differentiating with respect to radius and evaluating the dimensionless form at r_m results in

$$\left(\frac{\mathrm{d}\rho_u^*}{\mathrm{d}r^*}\right)_m = \left(\frac{\mathrm{d}p^*}{\mathrm{d}r^*}\right)_m - \left(\frac{\mathrm{d}T^*}{\mathrm{d}r^*}\right)_m \tag{48}$$

where an expression for the derivative of p^* at r_m can immediately be obtained from Eq. (32) as

$$\left(\frac{\mathrm{d}p^*}{\mathrm{d}r^*}\right)_m = \gamma_m M_{\mathrm{tm}}^2 (1 + w_m) \tag{49}$$

Finally, to capture the contribution from the change in opacity, the value of the Rosseland mean opacity [5] κ_r can be represented up to 10,000 K very accurately by a power law of the form $\kappa_r = aT^b$, with $a = 0.001371$ and $b = 1.585$, where the temperature is in Kelvin and the opacity is in m^2/kg. The slope of the opacity at r_m then becomes

$$\left(\frac{\mathrm{d}\kappa_r^*}{\mathrm{d}r^*}\right)_m = 1.585\left(\frac{\mathrm{d}T^*}{\mathrm{d}r^*}\right)_m \tag{50}$$

Pulling these expressions together, the derivative of λ_r^* is given in the final form as

$$\left(\frac{\mathrm{d}\lambda_r^*}{\mathrm{d}r^*}\right)_m = 2.415\left(\frac{\mathrm{d}T^*}{\mathrm{d}r^*}\right)_m - \gamma_m M_{\mathrm{tm}}^2 (1 + w_m) \tag{51}$$

Although the second term will depend on the selected values of M_{tm} and w_m, the first term is fixed by the value of $\mathrm{d}T^*/\mathrm{d}r^*$ at r_m for the case of the maximum heating value to roughly -10. The second term is of the same order, and because it is also negative, the overall value negative.

Referring now back to the equation for g_{fiss_m}, it is rewritten by taking the absolute value of all known negative terms and changing their signs to yield

$$g_{\mathrm{fiss}_m} = g_{\mathrm{rad}_m}\left|\frac{\mathrm{d}^2T^*}{\mathrm{d}r^{*2}}\right|_m + \left\{\frac{c_{p_m}}{\mathcal{R}} + g_{\mathrm{rad}_m}\left[1 - \left|\frac{\mathrm{d}\lambda_r^*}{\mathrm{d}r^*}\right|_m\right]\right\}\left|\frac{\mathrm{d}T^*}{\mathrm{d}r^*}\right|_m \tag{52}$$

where the fact that the second derivative of the temperature profile is negative at r_m is also used. Examining this expression, it can be seen that all of the terms contribute to a positive value of maximum fission rate except for one. Each of the positive terms represents a mechanism that removes heat locally from the system. The first term is the conduction of heat due to radiation, and because the heat flux increases in the direction of decreasing temperature (negative second derivative) there is always more heat conducting out of an element of volume than into it. Similarly, the first term in the curly brackets represents heat convection due to mass flow. Because the mass flows inward, from cooler to hotter regions, there is again always more energy leaving a volume element than entering it. The convective-type radiation term, however, is just the opposite. Although there is a small contribution of heat removal due to the cylindrical geometry (the "1" in the square brackets), the majority of the radiation transport is in the opposite direction. The convection of heat through radiation is strongly proportional to the slope of the temperature, and as a result more heat is caused to convect into the fluid element than out of it. This local heating is then in direct competition to what is allowable by the fission, if the condition on the temperature slope is to be maintained.

Because of the existence of a maximum heating value, and a competition to provide it, a crossover point will exist where heat addition due to fission will be forced to contribute less significantly than radiation. In the limit, this condition can be identified as the point where the contribution due to fission goes to zero. Grouping the terms proportional to g_{rad_m} in Eq. (52), results in

$$0 = g_{\mathrm{rad}_m}\left\{\left|\frac{\mathrm{d}^2T^*}{\mathrm{d}r^{*2}}\right|_m + \left[1 - \left|\frac{\mathrm{d}\lambda_r^*}{\mathrm{d}r^*}\right|_m\right]\left|\frac{\mathrm{d}T^*}{\mathrm{d}r^*}\right|_m\right\} + \frac{c_{p_m}}{\mathcal{R}}\left|\frac{\mathrm{d}T^*}{\mathrm{d}r^*}\right|_m \tag{53}$$

Inside the curly brackets, the second derivative of the temperature is only of order 1 (verified numerically), whereas the product of the term in square brackets with the temperature gradient is of order 10. Neglecting the "1" in the square brackets compared with the derivative of λ_r^* results in the following condition for zero allowable fission heat input

$$g_{\mathrm{rad}_m}\left|\frac{\mathrm{d}\lambda_r^*}{\mathrm{d}r^*}\right|_m = \frac{c_{p_m}}{\mathcal{R}} \tag{54}$$

and expanding g_{rad_m} in terms of the local gas properties gives

$$\frac{2\pi}{|\mathcal{M}|\mathcal{R}}\left(\frac{16\sigma T^3}{3\rho_u\kappa_r}\right)_m\left|\frac{\mathrm{d}\lambda_r^*}{\mathrm{d}r^*}\right|_m = \frac{c_{p_m}}{\mathcal{R}} \tag{55}$$

The dependence of ρ_u, κ_r, and $\mathcal{M}$ at r_m is repeated here as follows:

$$\rho_{u_m} \approx w_m m_H \frac{p_m}{\mathcal{R}T_m} \tag{56}$$

$$\kappa_{rm} = aT_m^b \tag{57}$$

$$\mathcal{M} = -2\pi\gamma M_{\mathrm{tm}}^2 \frac{m_U}{m_H}(\rho D_{12})_m \tag{58}$$

and inserting these into Eq. (55) yields

$$\frac{T_m^2}{p_m w_m} \approx \frac{1}{3}\left(\gamma_m + \frac{10}{(1+w_m)M_{\mathrm{tm}}^2}\right)^{-1} \tag{59}$$

where the MKS values of the constants have been inserted. This shows that to increase the operating temperature of the system, an increase must be made in the pressure, the uranium loading or the tangential Mach number at r_m. The performance implications of this relationship can be observed by relating this temperature to the specific impulse of the system. Although the temperature continues to increase somewhat beyond the value at r_m, the low fuel density and short dwell time of the propellant inside this radius mean that most of the heating has already occurred, and T_m is very near what the core temperature would be. Assuming full expansion through the nozzle, the specific impulse is given as

$$I_{\mathrm{sp}} = \frac{1}{g}(2c_p T_m)^{1/2} \tag{60}$$

and inserting the relationship for T_m given above

$$I_{sp} \approx \left(\frac{2c_p}{g^2}\right)^{1/2}\left[\frac{p_m w_m}{3}\left(\gamma_m + \frac{10}{(1+w_m)M_{tm}^2}\right)^{-1}\right]^{1/4} \tag{61}$$

showing that the specific impulse is a very weak function of the above mentioned parameters.

As a first approximation, the proper order of magnitude values of each of these parameters are inserted. These are $p_m \approx 10^7$ Pa, $w_m \approx 10$, and $M_{tm} \approx 1$. Assuming that in the best case the propellant is fully dissociated, this results in an expected specific impulse of only about 1300 s. In actual practice, the pressure can be maintained at 300 atm, and the Mach number would be less than one, resulting in a specific impulse of just over 1500 s. Although this is about 75% better than what can be achieved by a solid core system, it falls below what was anticipated by implementing the gas core. It is, of course possible to increase the performance level by increasing the pressure of the system, which will also have benefits in reducing the overall system mass. However, because of the weak dependence on the pressure, significant increases in pressure are necessary to get somewhat marginal increases in performance. As an example, increasing the pressure by a factor of 10 would be necessary to again improve performance by about 75%. This would bring the specific impulse to 2700 s. Increasing the value of w_m also proves ineffective in actually increasing the specific impulse, as it has the consequence of introducing greater pressure loss across the vortex, almost exactly negating any potential benefit.

It should be noted that in the preceding analysis, the number "10" that appears in Eq. (59) is actually an approximation to $16 - 4b$, where b is the power law chosen to fit the opacity below 10,000 K. Above this temperature, the opacity levels off to a peak value that depends on the pressure, and then begins to drop almost as rapidly as it rose [5]. Through this transition, the value of b essentially goes to zero and then becomes increasingly negative. The details of how the power law changes with temperature on the high side of 10,000 K are not important, because lowering the value of b in Eq. (61) results in the value "10" becoming larger, ultimately reducing the performance to below what has already been demonstrated.

Constraining Free Parameters

From the above analysis, the characteristics of the vortex have been reduced to a set of ten parameters: p_m, T_m, r_m, w_m, MHD, $\mathcal{M}$, M_{tm}, J_m, $g_{frac} = g_{fiss}/g_{fiss_m}$, and B. The truly dimensionless formulation of Kerrebrock and Meghreblian is lost by the introduction of multiple species in thermodynamic equilibrium, as it brings with it transcendental equations that do not allow complete removal of the reference values. For this reason, the temperature, pressure, and radius at peak fuel concentration remain as parameters to be specified. With further analysis of the physical system, some of these parameters can be related to others, or specified outright.

Physical Considerations

It is first noted from Eq. (30) that the MHD parameter has the direct influence of establishing the Mach number distribution across the vortex. It was shown that because of the mixing at the inlet, the velocity there is small, and the Mach number is essentially zero due to the high temperature. Also from Eq. (30) it can be seen that by setting M_t at the periphery to zero, the MHD parameter and dimensionless radius are uniquely related. Thus, by choosing the proper value of MHD, the Mach number will go to zero at the same radius that T_p reaches the desired wall temperature, avoiding conductive heat transfer to the wall. This condition cannot be satisfied a priori (without iteration), but in the parametric study, only examples where it is satisfied will be considered.

The relationship giving mass flow rate in terms of tangential Mach number and temperature at the reference radius still holds, and in a slightly modified form (due to dissociation), is found as before by solving Eq. (35) for the mass flow rate, and expressing v_m in terms of M_t. This results in

$$\mathcal{M} = -2\pi(\rho_1 D_{12})_m\left[\frac{m_2}{2-y} - 1\right]\gamma_m M_{tm}^2 \tag{62}$$

and noting that the product $(\rho_1 D_{12})_m$ is a function of temperature only, the dependence of the mass flow rate can be reduced to the form

$$\mathcal{M} = -K_m T_m^{1/2} M_{tm}^2 \tag{63}$$

where K_m is a constant depending on the mixture properties at the peak uranium concentration. This shows that the achievable mass flow rate is a weak function of the temperature and a strong function of tangential Mach number. It cannot, therefore, be specified independently.

When considering the electric current flow maintainable within a given vortex chamber, account should be taken as to how, and from where, the current will be supplied. The current leaves the cathode by the process of thermionic emission, which is a function of the material work function and temperature, given by

$$J_p = \frac{e}{4}\left(\frac{8kT}{\pi m_e}\right)^{1/2}\left(\frac{2\pi m_e kT}{h^2}\right)^{3/2}\exp(-e\phi/kT) \tag{64}$$

and is derived from the equilibrium flux of electrons to a surface of potential ϕ. This gives an upper bound to the electric current available based on the maximum allowable cathode temperature (assuming the cathode and the gas are at approximately the same temperature), and can be used to set the value of J based on this temperature.

Because of the freedom provided by the number of parameters available, it is possible to find many combinations of values that will achieve similar system performance levels. It is not obvious for some parameters, whether their values should be driven higher or lower, hence analysis of system performance under variations of these parameters must be undertaken. However, three of the parameters (r_m, p_m, and T_m) can be set to reasonable values that need not be varied. First, in the case of p_m, there is no penalty in specifying the pressure as high as can be achieved. Two benefits of a higher chamber pressure are a smaller throat area (for a given mass flow rate) and a higher uranium density. Although some mass penalty is incurred due to the necessary increase in strength of the pressure vessel to house the core, the reduction in reactor mass with higher uranium loading is the stronger effect. For this analysis, the pressure at the reference radius will be set to 200 atm. This is consistent with what is attainable with today's technology and allows for pressure losses through the system.

To set r_m, it is noted that the lower limit on the size of the vortex is determined by the radiative heat flux from the core. Any chamber of order centimeters or above will contain this heat, provided the pressure is of the order 100 atm, and the uranium loading is sufficiently high. Earlier studies of response of the system to changes in the value of r_m showed almost no dependence on the value when varied by less than an order of magnitude, and so the value of r_m will be set arbitrarily to 2 cm for the calculations. However, to first order the resulting systems can be rescaled by several centimeters without significantly affecting the results.

Finally, any value of T_m specified should be achievable by varying the heating rate and the uranium loading. However, because of the radiation dilemma, a maximum temperature of only 5,000 K can be achieved using the current state-of-the-art, and for this reason will be selected as T_m. The maximum theoretical specific impulse that can be achieved by such a system is then 1500 s.

Optimization

Writing the magnitude of the electric potential across the vortex from the integral of the electric field using $J = \sigma(E - vB)$, one obtains

$$V = \int \frac{J}{\sigma}\,dr + \int vB\,dr \tag{65}$$

which, using Eq. (11), can be integrated to get

$$V = \frac{J_m r_m}{\bar{\sigma}} + B v_m r_m [1 + \text{MHD}]\alpha \tag{66}$$

where

$$\frac{1}{\bar{\sigma}} = \int_{r_c}^{r_p} \frac{\mathrm{d}r}{r\sigma} \tag{67}$$

Using the fact that $M_t = 0$ at the perimeter

$$\alpha = \ell_n \left(\frac{r_p^*}{r_c^*}\right) + \frac{1}{2}\left[1 - \left(\frac{r_c^*}{r_p^*}\right)^2\right] \tag{68}$$

where r_p^* and r_c^* are the dimensionless radii at the outer and inner sides, respectively, of the uranium distribution.

Because the MHD parameter contains within it the product of the current and the magnetic field, setting a small value of J_m will result in a large value of B for a given value of MHD, and vice versa. Under this constraint, a minimum exists for the electric potential across the vortex, and it may be worthwhile to explore this as a baseline. To minimize the electric potential, which has two terms dependent on the current and magnetic field separately, it is necessary to choose J_m and B in such a way that the two terms in the potential are equal. This is equivalent to constraining the potential by the MHD parameter and setting the derivative to zero. Using this result, many of the parameters can now be fixed by the following relationships

$$\begin{aligned} J_p^2 &= \frac{\mathcal{M}}{\pi r_m^2}\alpha\bar{\sigma}v_m^2(1 + \text{MHD})\text{MHD} \qquad B^2 = \frac{\mathcal{M}}{\bar{\sigma}\alpha\pi r_p^2} \\ V &= 2v_m\left(\frac{\mathcal{M}\alpha(1 + \text{MHD})\text{MHD}}{\pi\bar{\sigma}}\right)^{1/2} \\ \mathcal{P} &= 4\mathcal{M}\alpha v_m^2(1 + \text{MHD})\text{MHD} \end{aligned} \tag{69}$$

where J_m has been replaced using $\nabla \cdot \boldsymbol{J} = 0$ ($J_p r_p = J_m r_m$) and the relationship between the MHD parameter and the dimensionless radius.

An interesting result from the above analysis is found by first taking the ratio of the power per unit vortex length, and mass flow per unit vortex length, resulting in the energy per unit mass delivered by electrical power

$$\frac{\mathcal{P}}{\mathcal{M}} = 4\alpha v_m^2(1 + \text{MHD})\text{MHD} \tag{70}$$

This may then be compared with the energy per unit mass delivered by the entire system [$\frac{1}{2}(I_{\text{sp}}g)^2$]. Written in terms of the specific impulse, the ratio gives

$$\frac{P_{\text{elec}}}{P_{\text{thrust}}} = 6\alpha(1 + \text{MHD})\text{MHD}\left(\frac{v_m}{I_{\text{sp}}g}\right)^2 \tag{71}$$

Parametric Study

Having specified the values of r_m, p_m, and T_m, found MHD and $\mathcal{M}$ to be related to other parameters, and set J_m and B by minimizing the potential (or relating J to the cathode temperature), only three parameters remain to be specified. These are w_m, M_{tm}, and g_{frac}. Although arguments can be made as to why these parameters should, in general, be set to a range of values, there is no way to determine analytically what values would achieve the desired performance. For example, the relationship between the MHD parameter and the radius of the vortex tube cannot be implemented directly. To set this condition, values of w_m, M_{tm}, and g_{frac} are chosen, and successive values of the MHD parameter are tested until the tangential Mach number goes to zero at some value of the radius. This is the radius at which the wall is "placed," and the value of the temperature at this radius is compared against the desired wall temperature. If both are within a certain tolerance of one another, that configuration is kept as a viable system, otherwise it is discarded.

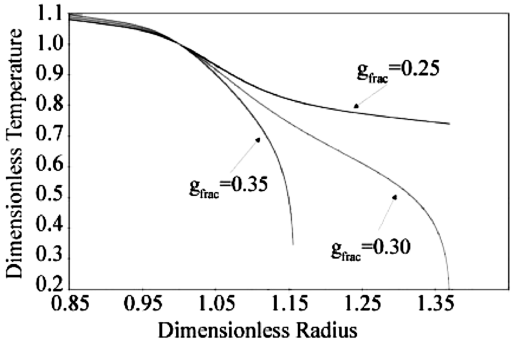

Fig. 5 Temperature profile variation with heating value.

Variations in the temperature profile are shown in Fig. 5 for different values of the heating value (g_{frac}). It can be seen that for high values of g_{frac}, the temperature becomes very steep, such that the change in the square root of the temperature (speed of sound) can occur more rapidly than the change in the flow velocity, causing the Mach number to rise suddenly near the wall. Examples of this phenomenon are shown in Fig. 6, where, starting from a viable system configuration, the heating value g_{frac} has been increased to cause the temperature to drop more rapidly near the perimeter. It is clear that at a heating fraction g_{frac} of 0.30, the Mach number falls almost linearly with increasing radius, but as the heating value is increased to 0.31, 0.32, and 0.33, the Mach number is made to increase closer to the reference radius, resulting from steeper temperature gradients.

Energy Transport

At this point, the approximation of eliminating the heat conduction from the energy equation can be justified. Figures 7 and 8 compare the contributions from the various heating mechanisms present in the system. The values for the heat conduction present were found by numerical evaluation of the term $\nabla \cdot (\lambda \nabla T)$, which, as in the case of the radiative transport, generates a term that appears with the convection terms (proportional to the temperature gradient) as well as a source term from the geometry (proportional to the second derivative). In Fig. 7, the source terms are shown as a function of radius, where each curve has been normalized to its maximum value in the domain (the maximum value is listed with the label for the curve.) The fission term dominates everywhere except below a radius of 0.90, where apparently, the radiation term dominates.

From the formula for λ_r, the conduction coefficient for radiation, one sees that the conductivity decreases with increasing density and opacity. This make physical sense, because higher collisionality between the photons and atoms would suggest an impedance to the

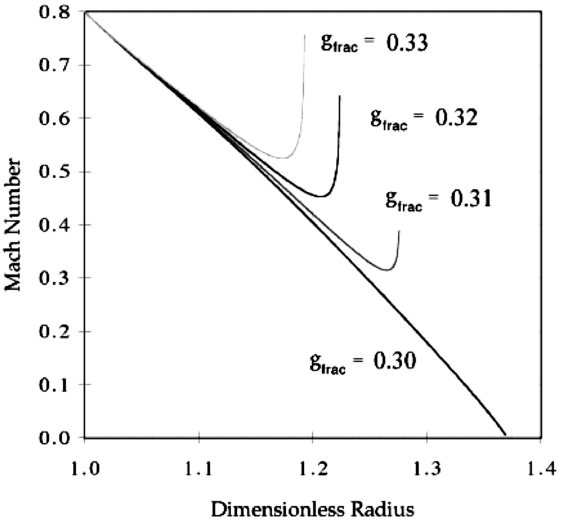

Fig. 6 Mach number curves for different heating fractions.

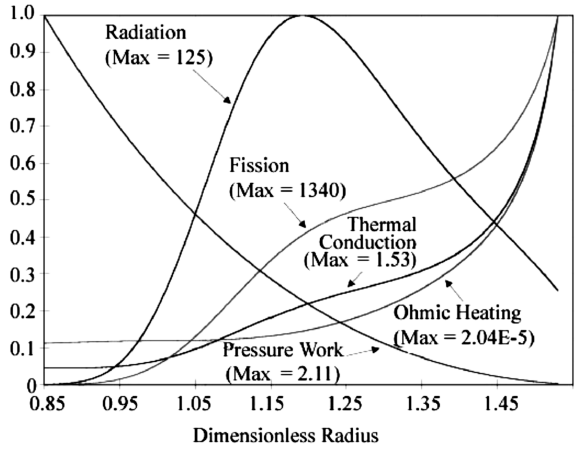

Fig. 7 Dimensionless volumetric heating rates.

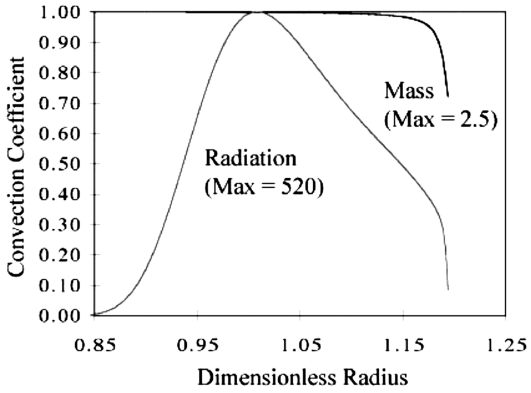

Fig. 8 Heat convection rates due to radiation and mass flow.

transfer of energy. However, as the density of the uranium decreases, the length scale over which the diffusion approximation is valid must increase. At some point the length scale for diffusion will become greater than that used for the numerical integration, and the solution will begin to diverge from physical reality. This is the case in the core of the vortex where very little uranium exists, and the gas need not be in equilibrium with the electromagnetic radiation. The low optical depth near the core would tend to indicate that the values in Fig. 7 are an overapproximation, and in fact the heating from the pressure gradient would probably dominate in this region.

In Fig. 8, the mass and radiation convection profiles are shown across the vortex, normalized by the gas constant for monatomic hydrogen, and then scaled to their maximum values (listed). The contribution from the mass flow is small (2.5) but constant over much of the domain, then drops off at the lower temperatures near the wall, where there is a greater abundance of H_2. The profile of the radiative heat convection rises (starting at the wall) as the cube of the temperature to its peak value (520), and then drops as the density of uranium (and hence the optical depth) decreases. Again, closer to the core of the vortex the result is somewhat artificial, in that a reduction in uranium density does not really "reduce the emissivity" as much as make the convection approximation invalid. However, the graph does show that heat convection due to radiation is actually dominant over convection due to mass flow. The characterization of the gas composition is then not directly needed to determine the heat flow characteristics over most of the system, but the distribution of uranium must be known to find the optical properties at each point.

Uranium Loading

The claim was made that higher uranium loading is desirable to reduce the overall mass of the system. The two methods of accomplishing this were to either increase the overall system pressure, or increase the amount of uranium relative to the propellant

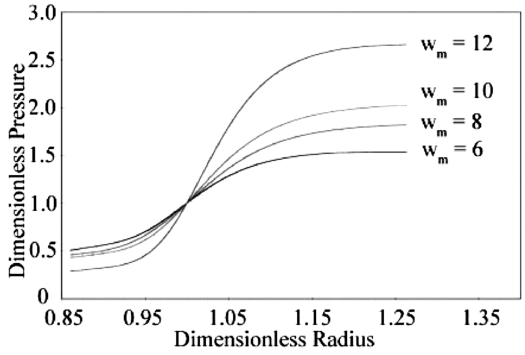

Fig. 9 Pressure distribution vs radius for different uranium loading.

at a constant pressure. The first method was employed by taking a base value of 200 atm to be the pressure at the reference radius, set to account for losses that would develop between there and the pump. Some loss is incurred upon injection of the propellant into the system, and then the pressure continues to fall as the gas diffuses inward through the uranium. This loss in pressure is shown in Fig. 9 for different values of w_m, ranging from 6 to 12. The effect of having a loss of pressure at the core is to reduce the mass flow rate that is achievable through a given throat area. Although the vortex mass flow rate per unit length is a function of M_{tm} and T_m (shown earlier), the total mass flow rate can in theory be increased by simply making the tube longer, and the aspect ratio achievable is then a function of the core pressure. Because higher uranium loading decreases reactor mass, but may also decrease thrust, a trade must be made after the final reactor geometry and layout are determined to see if there is a core pressure that would maximize this ratio, and if in fact it is important.

Another limiting factor on the uranium loading is its distribution across the vortex. For instance, for a subcritical heating value, the possibility exists of having an instability arise due to the density distribution in the vortex. Figure 10 shows examples of how the distribution varies as the heating value changes. At subcritical heating values ($g_{\text{frac}} = 0.25$), the distribution of uranium drops off to a low value near the wall. As the value of g_{frac} is increased, a second extremum occurs that indicates that the uranium fraction begins to rise again for increasing radius. The high molecular weight of the uranium means that these large variations in its distribution will have a profound effect on the overall density across the vortex.

The source of the instability that can arise is demonstrated in Fig. 11, where several cases are shown to have total density distributions that exhibit a maximum within the domain, due to the rapid drop in the uranium concentration in the direction of increasing radius (subcritical heating values). The situation that results is analogous to having two static fluids of different densities in a container. The acceleration of gravity establishes a pressure gradient in the fluids, with pressure increasing toward the bottom. Although an analysis of the static equilibrium of the system will not differentiate between the less dense liquid being on the bottom or top, only the latter configuration is dynamically stable, because otherwise a small perturbation at the interface will cause the fluids to trade

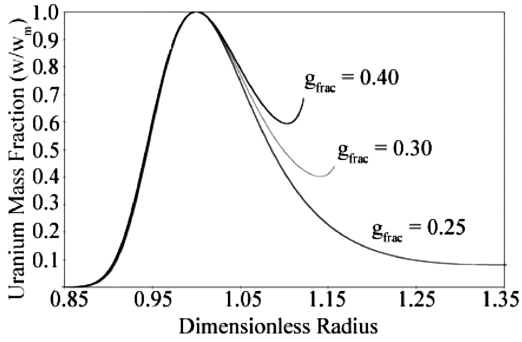

Fig. 10 Uranium distributions at various heating rates.

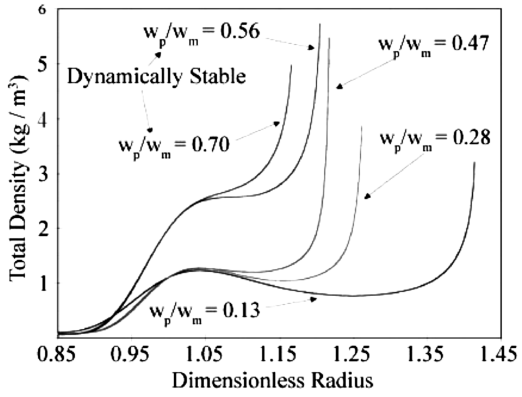

Fig. 11 Density variations leading to dynamic instabilities.

places. In the vortex chamber, the pressure decreases away from the wall, a result of the vortex flow, and therefore although this steady state analysis will allow for the situation where the density increases in this direction, in actual operation this would not be a stable configuration.

Because of the circulation present in the vortex, the requirement is even more stringent than merely having a monotonically increasing density in the radial direction, and a stability analysis yields that the condition on the density distribution is given by

$$\frac{\mathrm{d}\,\ell n\,\rho^*}{\mathrm{d}\,\ell n\,r^*} > 4 + \gamma M_{\mathrm{tm}}^2 \tag{72}$$

The cases in Fig. 11 are plotted for various values of w_p/w_m, the ratio of the uranium fraction between the periphery and the maximum. As a rule of thumb, fractions below 0.5 will not be stable (as shown), however, there is no way to identify these cases analytically and they must be discarded as each case arises.

Conclusions

Details of the 1-D Axisymmetric analysis of using MHD driven vortices for fuel containment have been presented. It was demonstrated that by the introduction of electromagnetic fields to a vortex tube, the vortex strength is uncoupled from the mass flow rate, allowing the propellant to be introduced at a much lower velocity at the outer wall, while still maintaining a quasistatic uranium distribution across the vortex. This same low velocity at the wall eliminates the problem of reduced diffusion resulting from turbulent mixing, and puts a constraint on the dimensionless radius of the tube, relating it to the MHD parameter. Additional free parameters were selected based on a number of physical arguments, and others were constrained by the choice of minimizing the electric potential across the vortex. A major finding of this research is the consequence of radiative heat transfer to the system. Concern has been expressed that over the small distances across the vortex (2–3 cm) an appreciable temperature gradient could not be maintained. It was found that in areas of high uranium concentration, a diffusion approximation to the radiative heat transfer could be made, and that direct escape of the radiation to the outer wall of the small diameter tubes turned out not to be a problem. However, a fundamental limit on the maximum heating rate, independent of the size of the tube, was found. The maximum system temperature appears to be limited to around 5000 K, above which uranium starts to accumulate near the outer wall. The result is that the specific impulse of the system is limited to around 1200–1500 s, well below the anticipated capability of the gas core system.

Acknowledgments

This research was funded in part by the Department of Defense through the U.S. Air Force Office of Scientific Research graduate research fellowship program, and in part by the Massachusetts Institute of Technology Department of Aeronautics and Astronautics. The authors would like to acknowledge Jack L. Kerrebrock for originating the concept, and thank him for his significant support and guidance in its analysis.

References

[1] Kerrebrock, J. L., and Meghreblian, R. V., "Vortex Containment for the Gaseous-Fission Rocket," *Journal of Aerospace Sciences*, Vol. 28, No. 9, 1961, pp. 710–724.

[2] Sedwick, R. J., "Analysis of an Open Cycle Gas Core Nuclear Propulsion System Using MHD Driven Vortices for Fuel Containment," Ph.D. Thesis, Department of Aeronautics and Astronautics, MIT, Cambridge, MA, 1997.

[3] Sedwick, R. J., and Zayas, D. A., "Magnetohydrodynamic Vortex Containment, Part 2: Equilibrium of Uranium Fluoride Fuel in Hydrogen Propellant," *Journal of Propulsion and Power*, Vol. 23, No. 1, 2007, pp. 90–98.

[4] Chapman, S., and Cowling, T. G., *The Mathematical Theory of Non-Uniform Gases*, Cambridge University Press, Cambridge, England, 1958.

[5] Parks, D. E., Lane, G., Stewart, J. C., and Peyton, S., "Optical Constants of Uranium Plasma," NASA CR-72348, GA-8244, Feb. 1968.

G. Spanjers
Associate Editor